NUMERICAL PREDICTIONS OF THE NONLINEAR BEHAVIOR FOR BI-AXIAL BRAIDINGS

J. Gager[1,2], H. E. Pettermann*[1]

[1] *Institute of Lightweight Design and Structural Biomechanics, Vienna University of Technology, A-1040 Vienna, Austria*

[2] *Polymer Competence Center Leoben GmbH, A-8700 Leoben, Austria*

* *Corresponding Author: pettermann@ilsb.tuwien.ac.at*

Keywords: modeling and simulation, CFRP braidings, nonlinear properties, damage and failure, plasticity

Abstract

Bi-axial ±45° *and* ±30° *carbon fiber reinforced polymer braidings are investigated with respect to their mechanical behavior including various modes of damage and plasticity. Nonlinear Finite Element predictions are carried out for a number of load cased up to laminate failure while monitoring the evolution of the material nonlinearities including the softening branch.*

The textile structure is represented by a plane periodic unit cell based on shell elements employing constitutive laws for the unreinforced polymer matrix material and the composite yarns. For the latter, an in-house developed constitutive model is used which includes plasticity and distributed damage.

Predictions are compared to experimental results for the same material system, which are carried out by cooperation partners.

1. Introduction

Braiding is a promising manufacturing technology for the automated production of continuously fiber reinforced composites components. Unless the component is cylindrical, local variations of the tow angles appear which results in spatial variations of the local composites properties. Moreover, such variations can be applied intentionally which offers some possibilities to materials tailoring.

For the application of composite components, computational predictions of their mechanical properties and performance are desired. Since the tow topologies inside a bi-axial braiding are similar to other textile composites, modeling approaches for e.g. weaves can be adopted.

The present paper utilizes periodic unit cell approaches to study the mechanical behavior of bi-axial braidings. First, the influence of the braiding angle on the initial elastic properties is investigated for a single layer featuring a 2/2 Twill type topology. Then, a ±45° and a ±30° braid is simulated including nonlinear tow behavior and the predictions are compared to corresponding experimental results obtained at the cooperation partners PCCL, *Polymer Competence Center Leoben GmbH, Austria (*`www.pccl.at`*)*, and LCC, *Chair of Carbon Composite, Technical University Munich, Germany, (*`www.lcc.mw.tum.de`*)*.

Table 1. Geometric dimensions of the lenticular tow cross section (Fig. 1), all values are given in mm.

Id	w	t	w_c	t_c	p	l_{UC}	f_{vol}
Braid-45	3.092	0.282	1.0	0.02	3.205	12.82	53.7%
Braid-30	2.749	0.311	0.19	0.042	2.968	11.87	47.7%

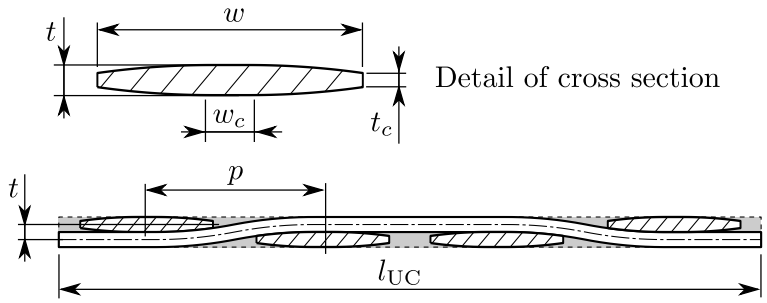

Figure 1. Cross section of a generic 2/2 Twill type braid featuring lenticular tow cross sections (hatched); the dashed line represents the unit cell perimeter and the gray areas denote the matrix pockets.

2. Modeling

To characterize the mechanical behavior of braided textiles in the perspective of material induced nonlinearities, a numerical approach based on homogenization of a periodic unit cell is applied. A modeling approach is utilized [1] by which all constituents are discretized with Finite Elements of shell type only, which are connected using surface based couplings. Master nodes (macroscopic degrees of freedom) are used to introduce the loads and to read the response of the unit cell.

Single layer unit cells are set-up using the lenticular tow cross section based approach presented in [2]. Four noded fully integrated shell elements with a Simpson type thickness integration (5 section points) and a typical element size of $1/12^{\mathrm{th}}$ of the tow width are used.
The loading conditions are applied in a force controlled way, as the underlying master node concept does not allow for the direct application of arbitrary loading states in a displacement controlled way. Since the reorientation of the material coordinate systems have a pronounced effect on the structural response geometrical nonlinear simulations are conducted.

2.1. Textile geometries

The modeling of general bi-axial braids start with an orthogonal ±45° braid. To achieve a non-orthogonal pattern, an affine transformation is used to generate unit cells representing braided textiles with braiding angles unequal 45° [3].
The present study focuses on 2/2 Twill type braids with ±30° and ±45° degrees braiding angle, respectively, featuring lenticular tow cross sections, see Figure 1. The textile geometry dimensions are listed in Tab. 1. Both are based on micrograph measurements conducted by the cooperation partner LCC using samples provided by PCCL.

2.2. Tow and Matrix Material

Braided textiles in structural application often feature a dense topology, i.e. there is no clearance between adjacent tows ($p \leq w$ cf. Fig 1). As the latter cannot be modeled by most (including the present) of the geometric representations, an open topology ($p \geq w$) is used to approximate the real textile. Therefore, the modeled unit cells feature a larger periodic length than the measured "real" specimens. This results in a lack of fiber volume fraction and thus, in a different overall mechanical response. To cope with this problem, the constituents material data is commonly scaled to achieve the required fiber volume fraction, see e.g. [4]. This procedure, also called "normalization", is strictly speaking nonphysical as the disability of the modeling approach is compensated with an artificial change of the material data, nevertheless, it is common practice. The scaling can be introduced based on various assumptions like linear correlation or micromechanical methods. In case of high volume fractions, micromechanical methods tend to give to high properties. Hence, for the current project a linear correlation between elastic material properties and fiber volume fraction is assumed. With this in mind, the two Young's moduli, the shear modulus and the (brittle) longitudinal tensile as well as compressive failure strength of the tow material are modified. All other properties are kept as originally defined.

The modeled ±45° unit cells feature a total fiber volume fraction of 53.7% based on a fiber volume fraction in the tows of 70%. The real ±45° braid was measured to features a total fiber volume fraction of 60%, hence, the tow fiber volume fraction has to be increased to 78%. Likewise, for the ±30° braid the total fiber volume fraction of 47% is achieved based on a tow fiber volume fraction of 70%. To aim at the measured total fiber volume fraction of 60%, the tow fiber volume fraction is increased to 88%. Correspondingly scaled material data is given in Tab. 2.
To incorporate material induced nonlinear effects, the tows are equipped with the *EPD-model* introduced in [7]. This material model allows for residual strain accumulation as well as stiffness degradation accompanied by strain hardening and strain softening, respectively. Additionally, viscous regularization helps to improve convergence of the numerical solution scheme. The unreinforced matrix pockets are represented using a linear elastic material, see Tab. 2. All interfaces are treated as being perfect.

3. Results

Due to the underlying elastic symmetries imposed by the braiding topology, the results are given with respect to the braiding coordinate system $\xi - \eta$, the first one being the braiding direction.

3.1. Elastic Properties

Assuming equal tow cross sections for all braiding angles (corresponding to the ±45° case), the initial stiffness properties of single layer braids featuring different braiding angles are predicted and juxtaposed.
Figure 2 shows the predicted polar plots of the initial Young's moduli (right) and shear moduli (left) of the braided composite. It can be clearly seen, that there is a significant influence of the braiding angle on the elastic constants . As expected lower braiding angles lead to higher stiffness in braiding direction and vice-versa. When comparing the shear moduli in braiding direction, $G_{\xi\eta}$, (Fig. 2 right), one would expect the ±45° braid to possess the highest value as

Table 2. Essential material data for the tows and matrix pockets of the RTM6/HTS40 material system scaled to 78% and 88% fiber volume fraction, original data based on [5, 6].

Tows (78 % fiber volume fraction)				
E_1	$E_2 = E_3$	$\nu_{12} = \nu_{13}$	ν_{23}	$G_{12} = G_{13}$
179.9 GPa	10.6 GPa	0.24	0.68	4.97 GPa
R^{t}_{11}	R^{c}_{11}	R^{t}_{22}	R^{c}_{22}	R_{12}
2631 MPa	1240 MPa	33 MPa	175 MPa	76.4 MPa
$\mathcal{G}_{(\mathrm{ft})}$	$\mathcal{G}_{(\mathrm{tc})}$	$\mathcal{G}_{(\mathrm{mt})}$	$\mathcal{G}_{(\mathrm{mc})}$	$\mathcal{G}_{(\mathrm{ps})}$
89800 J/m^2	78300 J/m^2	200 J/m^2	800 J/m^2	1000 J/m^2
Tows (88 % fiber volume fraction)				
E_1	$E_2 = E_3$	$\nu_{12} = \nu_{13}$	ν_{23}	$G_{12} = G_{13}$
203.2 GPa	11.99 GPa	0.22	0.68	5.61 GPa
R^{t}_{11}	R^{c}_{11}	R^{t}_{22}	R^{c}_{22}	R_{12}
2791 MPa	1400 MPa	33 MPa	175 MPa	76.4 MPa
$\mathcal{G}_{(\mathrm{ft})}$	$\mathcal{G}_{(\mathrm{tc})}$	$\mathcal{G}_{(\mathrm{mt})}$	$\mathcal{G}_{(\mathrm{mc})}$	$\mathcal{G}_{(\mathrm{ps})}$
89800 J/m^2	78300 J/m^2	200 J/m^2	800 J/m^2	1000 J/m^2
Matrix pockets				
E_{Matrix}	ν_{Matrix}			
2.89 GPa	0.38			

the shear loading in braiding direction can be transferred into a tensile-compressive loading in a 45° rotated coordinate system. However, the ±30° braid shows an even higher value.
Note that the ±30° and the ±60° braid are not only rotated cases of the same material. The braids' geometries are slightly different and so is the response. Simulations on multilayer braids have been shown in [2].

3.2. Nonlinear simulation of a ±45° single layer braid

The predicted stress-strain curves are compared with experimental results. The latter are supplied from the cooperation partner PCCL and are based on 8 layer specimens comprising the same ±45° braid, see [8]. Figure 3 shows the predicted response of the ±45° braid with respect to a uniaxial tensile load in braiding direction (black line) and a few experimentally determined curves (gray lines) in terms of nominal stresses and linearized strain. The black cross marks the point at which 1.5% of the total energy in the system is dissipated by the viscous regularization mechanism. This point is considered as the point of peak stress as the increase in viscous regularization energy indicates pronounced softening phenomena within the unit cell.

It can be clearly seen that with respect to this loading conditions the braid shows a pronounced nonlinear behavior. This nonlinearity can be attributed to the plasticity effects taking place in the tows. The overall trend of the simulated curve corresponds well with the experimental data. The prediction looks somewhat to compliant, however it matches one of the experimental curves quite perfectly, which suggests that the chosen, adapted, braid geometry represents a

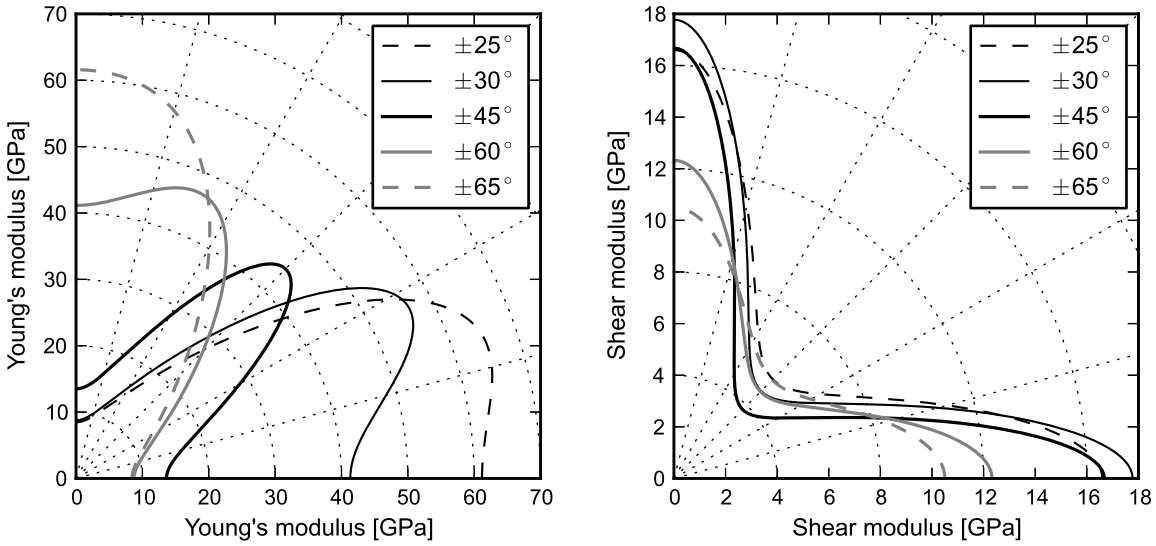

Figure 2. Polar plot of the predicted effective Young's modulus, E'_ξ (left) and the predicted effective shear modulus, $G_{\xi'\eta'}$ (right) for a single layer braid featuring a braiding angle of ±25°, ±30°, ±45°, ±60° and ±65°, respectively.

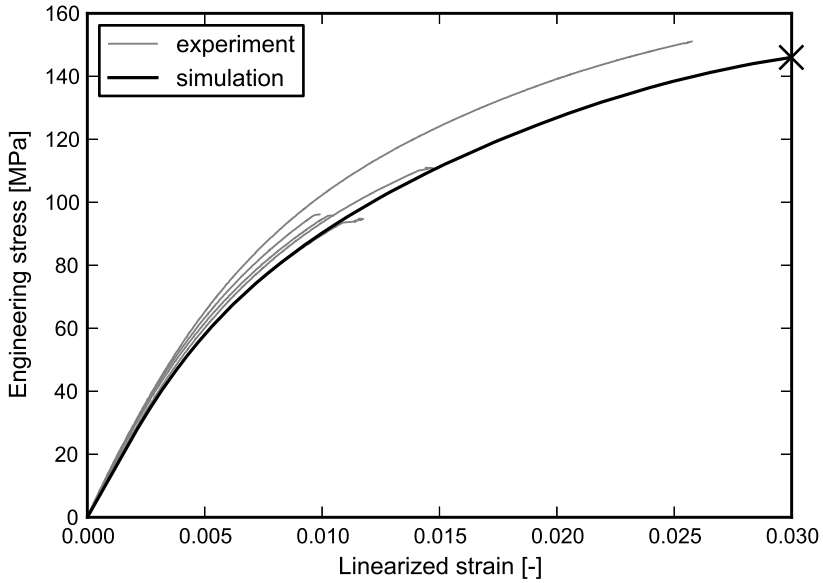

Figure 3. Predicted homogenized response of the ±45° braid unit cell due to macroscopic tensile stress, $\sigma_{\xi\xi}$, in braiding direction (black) compared to respective experimentally determined curves (gray). The black cross marks the predicted failure state.

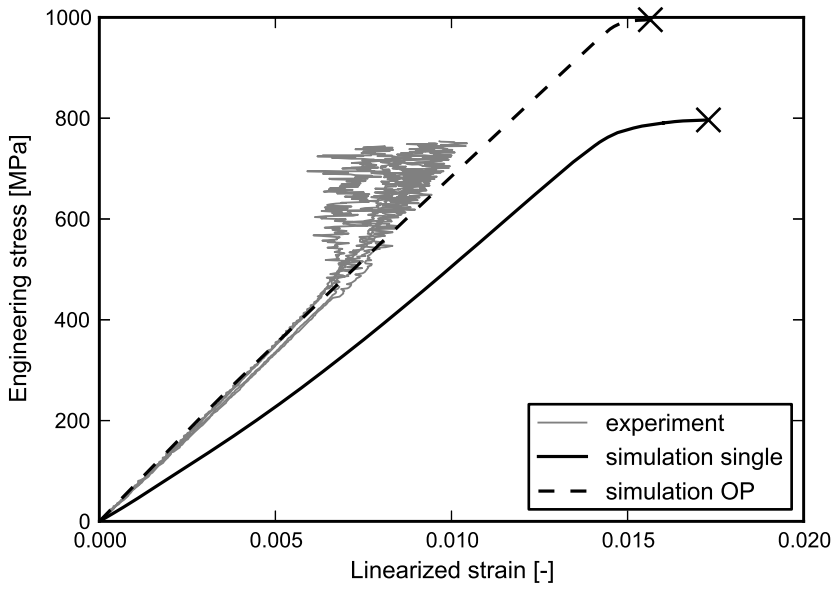

Figure 4. Predicted homogenized response of a free (black solid) and an OP-locked (dashed) single layer ±45° braid unit cell due to macroscopic uniaxial tensile stress in a tow direction, compared to respective experimental curves (gray).

rather compliant part of the investigated specimen. A statistical consideration of different tow cross sections may be appropriate here. The predicted failure load is in a good agreement with the maximum experimental failure load. Some of the experimental curves exhibit a failure load which is about 47% lower. The reason of the premature failure of those experiments is not known to the author, but could be caused by non-uniform load distribution within the specimens. During load increase the model develops large plastic zones all over the tows. Simultaneously, transverse tow damage appears at the cross over points but remains very localized. At elevated loads, this tow damage grows along the tows and, finally, leads to the failure of the unit cell.

The second considered load case is a uniaxial tensile loading along a tow direction. As shown in [2], loading of a braid in tow direction leads to local warping. However, the occurring of warping and, consequently, the response is highly dependent on the number of layers in the laminate. Hence, besides the simple (free) single layer simulation (Fig. 4, solid black line) a second simulation with locked out-of-plane displacements (OP) is conducted (dashed black line). The latter represents the extreme case of a laminate with an infinite number of out-of-phase stacked plies, see e.g. [9]. Figure 4 gives the predicted responses in terms of linearized stresses and engineering stresses juxtaposed with the experimental data (gray lines). The difference in initial stiffness of the two predicted curves can be clearly seen. The OP results are in a much better agreement with the experimental data, which indicates that within the laminate the local warping is significantly suppressed. The predicted failure strength for the free model is in good agreement with the experimentally determined strength. The increased strength of the OP case may be explained by the prevented local tow bending due to the additional boundary conditions. The latter effect is an artefact of the current modeling approach. For both simulation models the failure sequence is similar. At about 0.4% strain the tow normal to the loading direction starts to degrade in transverse direction. When reaching about 1.5% strain these tows split parallel to the fibers and concurrently the tows in loading direction start to fail.

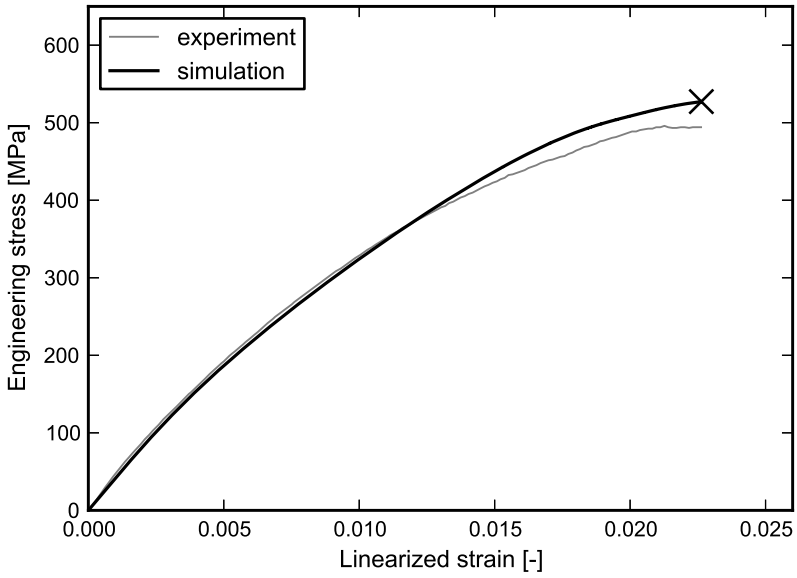

Figure 5. Predicted homogenized response of the ±30° braid unit cell due to macroscopic uniaxial tensile stress in braiding direction compared to an experimentally determined curve.

3.3. Nonlinear simulation of a ±30° single layer braid

In this section the response of a ±30° braid is investigated. To this end the unit cell is subjected to uniaxial tensile loads in and perpendicular to the braiding direction as well as in tow direction and the respective results are compared with experimentally determined ones.

The experimental results are taken from [10] and are determined from a 5 layer laminate of the same braid being defined as *Braid-30* in Tab. 2. The first considered load case is uniaxial tensile stress in braiding direction. As this loading state does not lead to local warping, only a free single layer simulation is conducted. Figure 5 shows the predicted linearized strain vs. engineering stress response of the ±30° braid (black line) compared to the experimental result (gray line). In general the curves are in an excellent agreement, even though the predicted failure strength is about 7% off. At the same time, the predicted failure strain matches the experimentally determined one very well.

The second investigated load case is uniaxial tensile stress in a tow direction. As discussed in the previous section, two predictions are presented, one for a free single layer and one for an OP-constrained layer. Figure 6 shows the respective effective responses compared with the experimental results. Again, the free layer possesses a far to low initial stiffness, but at higher strains the stretching of the tows lead to a predicted tangential stiffness which corresponds very well with the experimental value. The OP results are somewhat to stiff at the beginning but fit quite well at higher strains. Both results can be explained by the fact that a 5 layer laminate still exhibits some local warping flexibility and hence, shows some stiffening behavior. The predicted failure strength of the free layer model is in a good agreement with the experimentally obtained one. Again, the OP model shows a to high strength as no local tow bending can appear. The failure sequence highly resembles that of the ±45° braid, but this time also plasticity appears. Shear deformation is induced in the unit cell, since the loading direction is not a

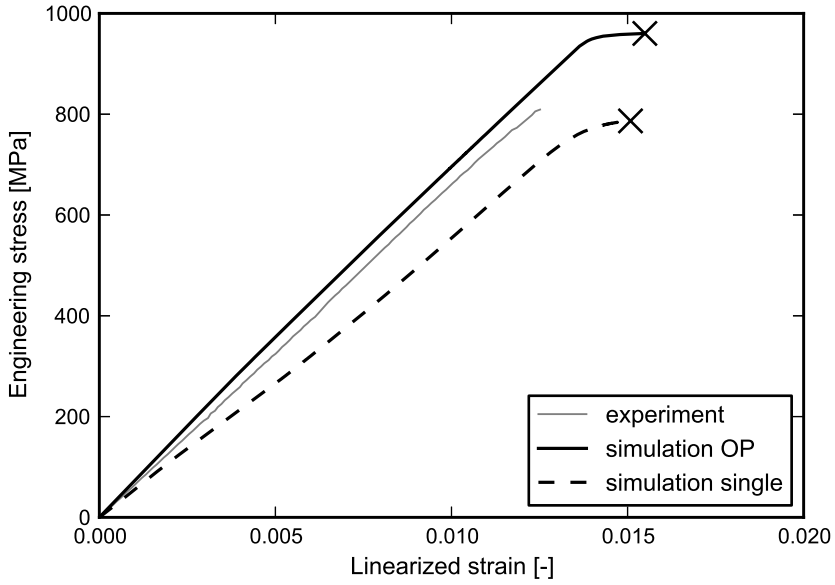

Figure 6. Predicted homogenized response of the ±30° braid unit cell due to macroscopic tensile stress, $\sigma_{\xi'\xi'}$, in x, i.e. a tow direction, compared to a respective experimentally determined curve.

principal axis of orthotropy.

The third considered loading situation represents a uniaxial tensile load perpendicular to the braiding direction. Again, this loading state does not lead to local warping, thus, only a free single layer simulation is conducted. Figure 7 shows the predicted effective response in terms of linearized strains and engineering stresses compared with an experimentally determined result. The initial stiffness still matches but starting at about 5 MPa the two responses deviate from each other. The unit cell gets to compliant and fails at about 50% of the experimental failure stress and strain. This pronounced difference can be explained by the perfect interface assumption in conjunction with touching tows applied within the shell element based modeling approach. The ±30° braid loaded perpendicular to the braiding direction tends to reorient the tows with respect to the loading direction. In the present model this scissoring can only be represented by shear deformation of the tows. In reality, however, the interfaces may break or intermediate matrix areas may deform plastically. Thus, the model is locally to stiff and gives rise to premature local damage which reduces global stiffness and strength. The predicted failure mode is attributed to tow failure in transverse direction whereas experiments show a shear-off of the tows, see [10]. To cope with this problem degradable interfaces within the unit cell could be incorporated.

4. Conclusion

The shell element based unit cells of bi-axial braided composites are shown to be able to accurately predict the stiffness and nonlinear response due to plasticity and damage in the tows. At the same time, the required simulation times and hardware specifications is significantly lowered. This performance gain allows for the simulation of explicitly modeled multilayer textiles as well as nonlinear simulations of the degradation and failure of respective braids. A comparison with experimental results reveal the good agreement with respect to stiffness and failure load predictions.

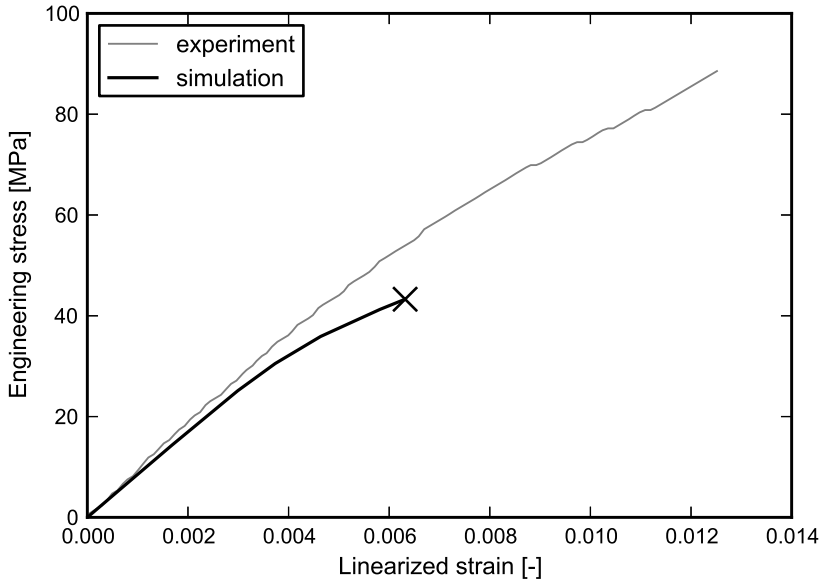

Figure 7. Predicted homogenized response of the ±30° braid unit cell due to macroscopic uniaxial tensile stress perpendicular to the braiding direction compared to a respective experimentally determined curve.

Acknowledgment

The funding of the Polymer Competence Center Leoben GmbH (PCCL, Austria) within the framework of the COMET-K1-program of the Austrian Ministry of Traffic, Innovation, and Technology and the Austrian Ministry of Economics and Labor is gratefully acknowledged.

References

[1] J. Gager and Heinz E. Pettermann. Numerical homogenization of textile composites based on shell element discretization. *Composites Science and Technology*, 72(7):806–812, 2012.

[2] J. Gager. *Modeling and simulation concepts for advanced braided composites*. PhD thesis, Vienna University of Technology, Austria, 2013. (also published as: VDI Fortschritt-Berichte VDI Reihe 18 Nr. 338. VDI-Verlag, Düsseldorf).

[3] D. Goyal, X. Tang, J. D. Whitcomb, and A. D. Kelkar. Effect of various parameters on effective engineering properties of 2 × 2 braided composites. *Mechanics of Advanced Materials and Structures*, 12(2):113–128, 2005.

[4] K. M. Charlebois, R. Boukhili, O. Zebdi, F. Trochu, and A. Gasmi. Evaluation of the physical and mechanical properties of braided fabrics and their composites. *Journal of Reinforced Plastics and Composites*, 24(14):1539–1554, 2005.

[5] C. Schillfahrt. Bestimmung ausgewählter mechanischer Eigenschaften sowie der monotonen und zyklischen interlaminaren Risszähigkeit von gewickelten und geflochtenen Kohlenstofffaserverbundwerkstoffen. Master's thesis, Montanuniversitaet Leoben, 2012.

[6] M. Schubert. Vergleich eines Resin Transfer Moulding Expoxidharzsystems mit einem Prepregharzsystem. In *17. Symposium "Verbundwerkstoffe und Werkstoffverbunde" der DGM*, Bayreuth, Germany, 2009.

[7] Th. Flatscher and H. E. Pettermann. A constitutive model for fiber-reinforced polymer plies accounting for plasticity and brittle damage including softening - implementation for implicit FEM. *Composite Structures*, 93(9):2241–2249, 2011.

[8] J. Cichosz, J. Bückle, R. Hinterhölzl, and Wolfahrt M. Predicting the constitutive behavior of biaxial braided composites using beam unit cells. In *Proceedings of the 19th International Conference on Composite Materials (ICCM19)*, page 9, Montreal, Canada, 2013.

[9] N.V. De Carvalho, S.T. Pinho, and P. Robinson. Numerical modelling of woven composites: Biaxial loading. *Composites Part A: Applied Science and Manufacturing*, 43(8):1326–1337, 2012.

[10] J. Cichosz, P. Huber, and R. Hinterhölzl. Off-axis testing of biaxial braided composites. In *Proceedings of the TEXCOMP-11 CONFERENCE*, Leuven, Belgium, 2013.